AEM
Journals.ASM.org

Novel Broad-Spectrum Antimicrobial Photoinactivation of *In Situ* Oral Biofilms by Visible Light plus Water-Filtered Infrared A

L. Karygianni,[a] S. Ruf,[a] M. Follo,[b] E. Hellwig,[a] M. Bucher,[a] A. C. Anderson,[a] K. Vach,[c] A. Al-Ahmad[a]

Department of Operative Dentistry and Periodontology, Center for Dental Medicine, Albert-Ludwigs-University, Freiburg, Germany[a]; Department of Hematology and Oncology, Core Facility, Albert-Ludwigs-University, Freiburg, Germany[b]; Institute for Medical Biometry and Statistics, Center for Medical Biometry and Medical Informatics, Albert-Ludwigs-University, Freiburg, Germany[c]

Antimicrobial photodynamic therapy (APDT) has gained increased attention as an alternative treatment approach in various medical fields. However, the effect of APDT using visible light plus water-filtered infrared A (VIS + wIRA) on oral biofilms remains unexplored. For this purpose, initial and mature oral biofilms were obtained *in situ*; six healthy subjects wore individual upper jaw acrylic devices with bovine enamel slabs attached to their proximal sites for 2 h or 3 days. The biofilms were incubated with 100 μg ml^{-1} toluidine blue O (TB) or chlorin e6 (Ce6) and irradiated with VIS + wIRA with an energy density of 200 mW cm^{-2} for 5 min. After cultivation, the CFU of half of the treated biofilm samples were quantified, whereas following live/dead staining, the other half of the samples were monitored by confocal laser scanning microscopy (CLSM). TB- and Ce6-mediated APDT yielded a significant decrease of up to 3.8 and 5.7 log$_{10}$ CFU for initial and mature oral biofilms, respectively. Quantification of the stained photoinactivated microorganisms confirmed these results. Overall, CLSM revealed the diffusion of the tested photosensitizers into the deepest biofilm layers after exposure to APDT. In particular, Ce6-aided APDT presented elevated permeability and higher effectiveness in eradicating 89.62% of biofilm bacteria compared to TB-aided APDT (82.25%) after 3 days. In conclusion, antimicrobial photoinactivation using VIS + wIRA proved highly potent in eradicating oral biofilms. Since APDT excludes the development of microbial resistance, it could supplement the pharmaceutical treatment of periodontitis or peri-implantitis.

Recent years have seen intensified attempts in microbiological research to eliminate dental plaque biofilms, the most persistent microbial community in the oral cavity. This is due to the fact that biofilm-associated infections such as caries, periodontal disease, and peri-implantitis are etiologically related to pathological shifts in the supragingival and subgingival dental plaque biofilms (1, 2). These microbial communities possess resilient survival capabilities due to complex intrabiofilm cell-cell communication channels. Among them, metabolic exchange, horizontal gene transfer via matrix-mediated endogenous or exogenous DNA, and quorum sensing in the presence of small molecules promote microbial adaptation to adverse environmental conditions (3). As a result, oral biofilm bacteria can be up to 1,000 times more resistant to chemotherapeutic agents, local antimicrobials, and host defense mechanisms than their planktonic counterparts (4, 5). Moreover, the favorable outcomes of mechanical biofilm detachment are often reversed by a tendency toward biofilm concealment at oral sites beyond reach, such as root canals with challenging anatomy, impassable furcation defects, and deep periodontal pockets (6). The treatment of polymicrobial dental infections is also challenged by intra- or interindividual disparities. Hence, the introduction of novel target-specific treatment approaches supplementary to the conventional therapeutic reservoir is considered crucial for the efficient control and eradication of biofilm-related oral diseases.

In view of the adverse outcomes in established oral biofilm treatments, the implementation of antimicrobial photodynamic therapy (APDT) paved the way for a compelling, noninvasive, biofilm-targeted, photochemical method which can be used against dental infections. At the outset of the 20th century, APDT as initially developed was used solely to target malignant and infected skin cells of the human body (7). Since then, its application spectrum has broadened to include dental therapeutic protocols, such as light-induced inactivation of periodontal pathogens or treatment of cancerous oral lesions, among others (8). APDT combines the use of a nontoxic local photosensitizer with an innocuous source of visible light and oxygen (9). Toluidine blue O (TB), methylene blue (MB), chlorin e6 (Ce6), hematoporphyrin, and erythrosine belong to the most used biodegradable cationic photosensitizing agents, capable of selectively infiltrating the cytoplasmic membrane of bacterial cells and yeasts upon activation by illumination (10). The action mode of APDT primarily involves the excitation of the photosensitizer to a high-energy triplet state. The latter subsequently interacts either with the organic substrate or with endogenous molecular oxygen via electron and hydrogen atom detachment, yielding reactive oxygen species (ROS), e.g., hydrogen peroxide (H_2O_2), superoxide ion (O_2^-) and free hydroxyl radical (·HO) (type I reaction). Alternatively, the reaction of the activated photosensitizer with molecular oxygen leads to the emergence of highly reactive singlet oxygen ($^1O_2$) (type II reaction) (11). As a result, protein or lipid disintegration and selective target destruction occur (12).

Regarding the light sources which can be used for APDT, the generation of harmless, low-power visible light at the longest

Received 28 July 2014 **Accepted** 13 September 2014
Published ahead of print 19 September 2014
Editor: A. M. Spormann
Address correspondence to L. Karygianni, lamprini.karygianni@uniklinik-freiburg.de.

doi:10.1128/AEM.02490-14

wavelength or wavelength range of the photosensitizer's absorption spectrum is a fundamental prerequisite. To date, various laser devices (argon, diode, or neodymium doped: yttrium, aluminum, and garnet [Nd:YAG] lasers) and nonlaser light generators (halogen or light-emitting diode [LED] lamps) have been utilized for APDT protocols (13). The monochromaticity and high performance potential of lasers, their high costs, and their limited applicability for photosensitizers with different maximum absorption peaks render the use of expensive, heavyweight, single-wavelength laser units unfavorable (14). Low-priced LED appliances also have a restricted emission wavelength spectrum, while wide-band halogen lamps can induce tissue overheating (13). Hence, the development of a broad-band light source which contains visible-light (VIS) wavelengths in combination with water-filtered infrared A (wIRA) wavelengths has ushered APDT into a new era. VIS + wIRA is portable, inexpensive, and highly flexible in terms of the photosensitizers which can be used (15). The main thermal effects of wIRA encompass increased tissue oxygen partial pressure, higher local temperature, and higher perfusion levels, thereby inducing chronic wound healing and pain reduction (16). Moreover, due to its significant subcutaneous tissue penetration, wIRA counteracts the immense thermal stress on the external tissue layers (17, 18). Lastly, the nonthermal impact of wIRA consists of enhanced antimicrobial properties in the presence of endogenous or bacterial protoporphyrin IX (19).

Even though APDT using VIS + wIRA and TB thoroughly eliminated the initial oral bacterial colonization *ex vivo* in a previous study carried out by our group, to date there are no clinical data on the antimicrobial impact of this technique utilizing different photosensitizers on *in situ*-grown initial and mature oral biofilms (20). In light of the established efficacy of APDT using VIS + wIRA and TB on initial oral bacterial adhesion, the rationale for the present study was to describe the treatment protocol for a novel experimental APDT approach with the use of VIS + wIRA, thereby assessing its effectiveness against *in situ*-formed initial and mature oral biofilms. For this purpose, intact oral biofilms grown *in situ* on bovine enamel slabs (BES) within the oral cavity for 2 h or 3 days, respectively, were treated with APDT using VIS + wIRA in the presence of either TB or Ce6 as a photosensitizer. In addition to determination of CFU, the treated biofilm was also visualized and quantified by live/dead staining. The results demonstrated significant eradication of oral biofilm bacteria using APDT. To the best of our knowledge, this is the first time that the effect of VIS + wIRA combined with TB or Ce6 has been tested on *in situ* initial and mature oral biofilms.

MATERIALS AND METHODS

Selection of study participants and test specimens. After giving their written informed consent, six healthy volunteers between 25 and 54 years of age participated in the study. The study protocol was reviewed and approved by the Ethics Committee of the University of Freiburg (no. 91/13). A thorough clinical oral examination was conducted prior to the experiments. DMFT (decayed, missing, filled teeth) values of 4.5 ± 3 were measured, saliva flow rates were estimated at 1.2 ± 0.3 ml/min, and lactate formation rates of 2.5 ± 0.6 (on a scale from 1 to 9) were detected. The following exclusion criteria applied to this study: (i) severe systemic disease, (ii) diseases of the salivary glands, (iii) presence of carious lesions or periodontal disease, (iv) pregnancy or lactation, (v) use of antibiotics or local antimicrobial mouth rinses such as chlorhexidine (CHX) within the last 30 days.

In order to prepare the test specimens, the buccal surfaces of the bovine incisors of freshly slaughtered 2-year-old cattle were detached and modified into cylindrical enamel samples (diameter, 5 mm; 19.63-mm^2 surface area; height, 1 mm), as has been described (21). Prior to tooth extraction, examination of cattle with the IDEXX laboratories bovine spongiform encephalopathy (BSE) diagnostic kit (Ludwigsburg, Germany) had confirmed the absence of BSE. Afterwards, the enamel surfaces of all specimens were polished by a wet grinding machine (Knuth-Rotor-3; Streuers, Willich, Germany) using sandpaper (abrasive grading scales from 250 to 4,000 grit) in decreasing order of grain size. The burnished bovine enamel slabs (BES) were then controlled under a light microscope (Wild M3Z; Leica GmbH, Wetzlar, Germany) and were finally cleansed. The disinfection protocol of BES involved ultrasonication in NaOCl (3%) for 3 min to wash off the superficial smear layer, air drying, and then ultrasonication in 70% ethanol for 3 min. The disinfected BES were then ultrasonicated twice in double-distilled water for 10 min and finally deposited in distilled water for 24 h to hydrate before application in the oral cavity (22).

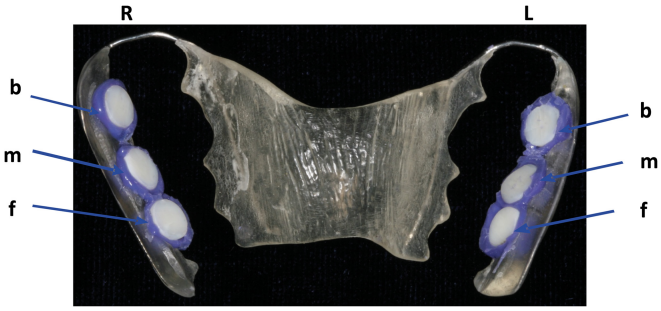

FIG 1 Individual upper jaw acrylic appliance with the enamel slabs placed in different locations. The specimens were positioned at the front (f), in the middle (m) and in the back (b), on both sides, right (R) and left (L), of the appliance. The exposed surfaces were attached to the tooth enamel with silicone.

Individual upper jaw acrylic appliances were fabricated for each study participant, and six BES were anchored on their proximal sites using an A-silicon compound (Panasil initial contact X-Light; Kettenbach GmbH & Co. KG, Eschenburg, Germany), as described elsewhere (22). In order to facilitate the exposure of the BES surfaces to the oral cavity, their margins were fully covered by the impression material (Fig. 1). The BES were subsequently fixed to the interdental area between upper premolars and molars, so that the movements of the tongue or cheek would not disturb biofilm formation in the following 2 h or 3 days. For each time period, every individual carried a total of 12 BES. Each participant wore the BES-incorporating acrylic appliances twice for each period to provide a sufficient number of BES for the APDT assays that followed.

Light source and photosensitizers. For the *ex vivo* assays, a broadband VIS + wIRA radiator (Hydrosun 750 FS; Hydrosun Medizintechnik GmbH, Müllheim, Germany) with a 7-mm water cuvette was used. In addition, an accessory orange filter, BTE 31, was adapted to the light generator. In contrast to the common orange filter BTE 595, the fitted BTE 31 filter allowed more than a doubled weighted effective integral irradiance in terms of the absorption spectrum of protoporphyrin IX. As a result of the absorption of water molecules, the continuous water-filtered spectrum covered a wavelength range from 570 nm to 1,400 nm, with local minima at 970 nm, 1,200 nm, and 1,430 nm (23). The unweighted (absolute) irradiance of 200 mW cm^{-2} VIS + wIRA was applied to the samples for 5 min, consisting of approximately 48 mW cm^{-2} VIS and 152 mW cm^{-2} wIRA.

The broadband light source used in this study allowed optimal light absorption by the applied photosensitizers. The photosensitizing agents used were toluidine blue O (TB) ($C_{15}H_{16}ClN_3S$; Sigma-Aldrich, Munich, Germany) and chlorin e6 (Ce6) ($C_{34}H_{36}N_4O_6$; Frontier Scientific, Logan, UT, USA). TB and Ce6 were diluted in 0.9% saline solution (NaCl) to a

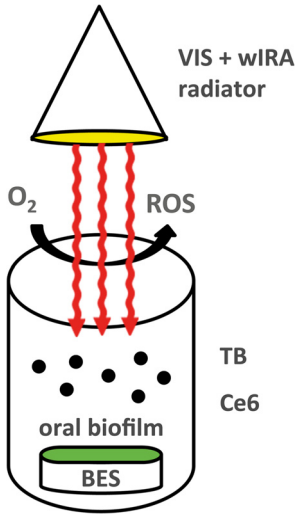

FIG 2 Schematic representation of antimicrobial photodynamic therapy using visible light (VIS) plus water-filtered infrared A (wIRA). Under the influence of a broadband VIS + wIRA radiator with a water-filtered spectrum in the range of 570 to 1,400 nm, the tested photosensitizers toluidine blue (TB) and chlorin e6 (Ce6) reached an excited-singlet state. Their activation led to an interaction with oxygen (O_2), which resulted in the production of various reactive oxygen species (ROS), like singlet oxygen. The latter are considered to intoxicate initially adherent microorganisms and resistant structures such as oral biofilms.

final concentration of 100 μg ml^{-1}. Prior to use, the freshly prepared TB and Ce6 solutions were kept in the dark at 4°C for no longer than 14 days to prevent any light-induced photochemical alterations. The optical absorption band of TB extended from 500 nm to 700 nm. The visible absorption maximum (λ_{max}) of TB was 630 ± 4 nm; λ_{max} of TB were also observed at 570 nm and 650 nm (24). The optical absorption measurement of Ce6 revealed maximum absorption peaks at around 403 ± 2 nm (Soret band) and 664 ± 3 nm (Q band), respectively (25).

APDT protocol for oral biofilms. Each volunteer carried an individual upper jaw acrylic appliance to which six BES were fixed for 2 h or 3 days. This procedure was performed twice for each subject and time period. After the oral biofilms had been obtained *in situ*, the BES were removed from the oral cavity. Sterile tweezers were used to detach the silicon from the samples, which were then rinsed off with sterile 0.9% NaCl for 30 s. Two specimens out of a total of six BES per participant served as controls. Specifically, one 0.2% CHX-treated plate was used as a positive control, and one untreated biofilm sample served as a negative control. The remaining four biofilm-covered BES were treated with APDT *ex vivo*. VIS + wIRA was applied to two of the BES in the presence of 100 μg ml^{-1} TB and to the other two BES with 100 μg ml^{-1} Ce6. For the application of APDT, the BES were placed in multiwell plates (24-well plate; Greiner bio-one GmbH, Frickenhausen, Germany) and incubated with the photosensitizers for 2 min in the dark, in duplicate. Afterwards, the VIS + wIRA radiation was applied for 5 min at 37°C (Fig. 2). Subsequently, the BES were transferred into multiwell plates with 1 ml 0.9% NaCl, and the adherent microorganisms were finally quantified by determination of the CFU. Additional biofilm samples were obtained from a second cycle for each time point and visualized by live/dead staining, as described below.

Quantification of the adherent oral biofilm microorganisms. In brief, sterile small foam pellets (Voco GmbH, Cuxhaven, Germany) were used to brush off the reverse dentine surfaces of the BES and their upright side margins. The BES were then washed with 1 ml 0.9% NaCl for 10 s to dislodge the nonadherent microorganisms, inserted into sterile Eppendorf tubes (Eppendorf GmbH, Wesseling-Berzdorf, Germany) with 1 ml 0.9% NaCl, ultrasonicated for 2 min in 1 ml NaCl on ice, and finally vortexed for 30 to 45 s to release the microorganisms from the surfaces. Afterwards, the suspensions of untreated BES (negative control) and CHX-treated BES were serially diluted up to 1:10^3 in 0.9% NaCl; an equivalent dilution series (10^{-1} to 10^{-3}) was also prepared for the treated BES. Subsequently, aerobic and facultative anaerobic bacteria were cultivated on Columbia blood agar plates (CBA; Becton Dickinson, Heidelberg, Germany) at 37°C and 5% to 10% CO_2 for 5 days. Anaerobic bacteria were cultivated on yeast-cysteine blood agar plates (HCB; Becton Dickinson, Heidelberg, Germany) at 37°C for 10 days (anaerobic chamber; Genbox bioMérieux SA, Marcy l'Etoile, France). The number of CFU per ml was determined using the Gel Doc EQ universal hood (Bio-Rad Life Science Group, Hercules, CA, USA). Each measurement was repeated twice.

Live/dead staining and CLSM. For the live/dead staining and confocal laser scanning microscopy (CLSM) assay, the fluorescent SYTO 9 stain and propidium iodide (PI) (Live/Dead BacLight bacterial viability kit; Life Technologies GmbH, Darmstadt, Germany) were used (26). The green fluorescence stain SYTO 9 can penetrate both intact and disrupted cell membranes. The latter are selectively permeable for red-fluorescent PI. Hence, viable bacterial cells fluoresce green, whereas damaged cells fluoresce red. At first, the fluorescent agents were diluted in a 0.9% NaCl solution to a final concentration of 0.1 nmol ml^{-1}. The biofilm-covered BES were then placed into multiwell plates and were stained with 1 ml SYTO 9–PI in 0.9% NaCl per well in a dark chamber for 10 min at room temperature. The stained BES were subsequently placed face down onto a drop of NaCl solution in a chambered cover glass (μ Slide 8 well; ibidi GmbH, Munich, Germany) and were then analyzed using CLSM (Leica TCS SP2 AOBS; Leica, Mannheim, Germany) with a 63× water immersion objective (model no. HCX PL APO/bd. BL, 63.0 × 1.2 W; Leica, Mannheim, Germany). For the quantification of oral biofilm vitality after the APDT, the obtained initial and mature biofilms were screened at three representative positions. In brief, for each experimental time period (2 h or 3 days), a total of 18 biofilm locations, namely, three positions for each of the 6 BES per subject, were examined. The upper and lower boundaries of the oral biofilm at each of the three selected locations were determined and used for the calculation of mean biofilm thickness. Afterwards, biofilms were scanned in the Z direction at these three points, yielding optical sections with a thickness of approximately 0.5 μm, each taken at 2-μm intervals throughout the biofilm layers. In order to minimize the risk of spectral overlap, sequential scanning was utilized. Each standard image was transformed into a digital image with a resolution of 1,024 × 1,024 pixels. The zoom setting was 1.7, corresponding to physical dimensions of 140 by 140 μm. The measurement was conducted in duplicate. Initial oral biofilms exposed solely to either TB or Ce6 in the absence of VIS + wIRA and served as supplementary controls for visualization. Representative images were acquired for demonstration of the results.

Image analysis. Image analysis was performed as described elsewhere (27). The program LSM Image Browser (Zeiss, Oberkochen, Germany) was utilized to yield the maximal projection of each image stack and, hence, to quantify the covering grades of the scanned biofilm points. The red-and-green projections were then converted into merged black-and-white (B/W) images by the image analysis program MetaMorph 6.3r7 (Molecular Devices Corporation, Sunnyvale, CA, USA), and B/W intensity thresholds were manually set for each of the measured biofilm regions to define the total surface area colonized by viable and nonviable microorganisms. The statistical significance of the resulting covering grades of live and dead cells (percent positive within the total scanned biofilm region) was further analyzed.

Statistical analysis. For a descriptive evaluation of the data, the means and standard deviations were computed. A Friedman test was used to check for overall differences between the test groups regarding the microbial load. A *t* test with a Bonferroni correction (multiple testing) was used for pairwise group comparisons, due to the limited power of a nonparametric test related to small sample size. Diagrams of the viable bacterial counts on the $\log_{10}$ scale per square centimeter ($\log_{10}$/cm^2) were graphically displayed, stratified by biofilm age (initial/mature) and type of mi-

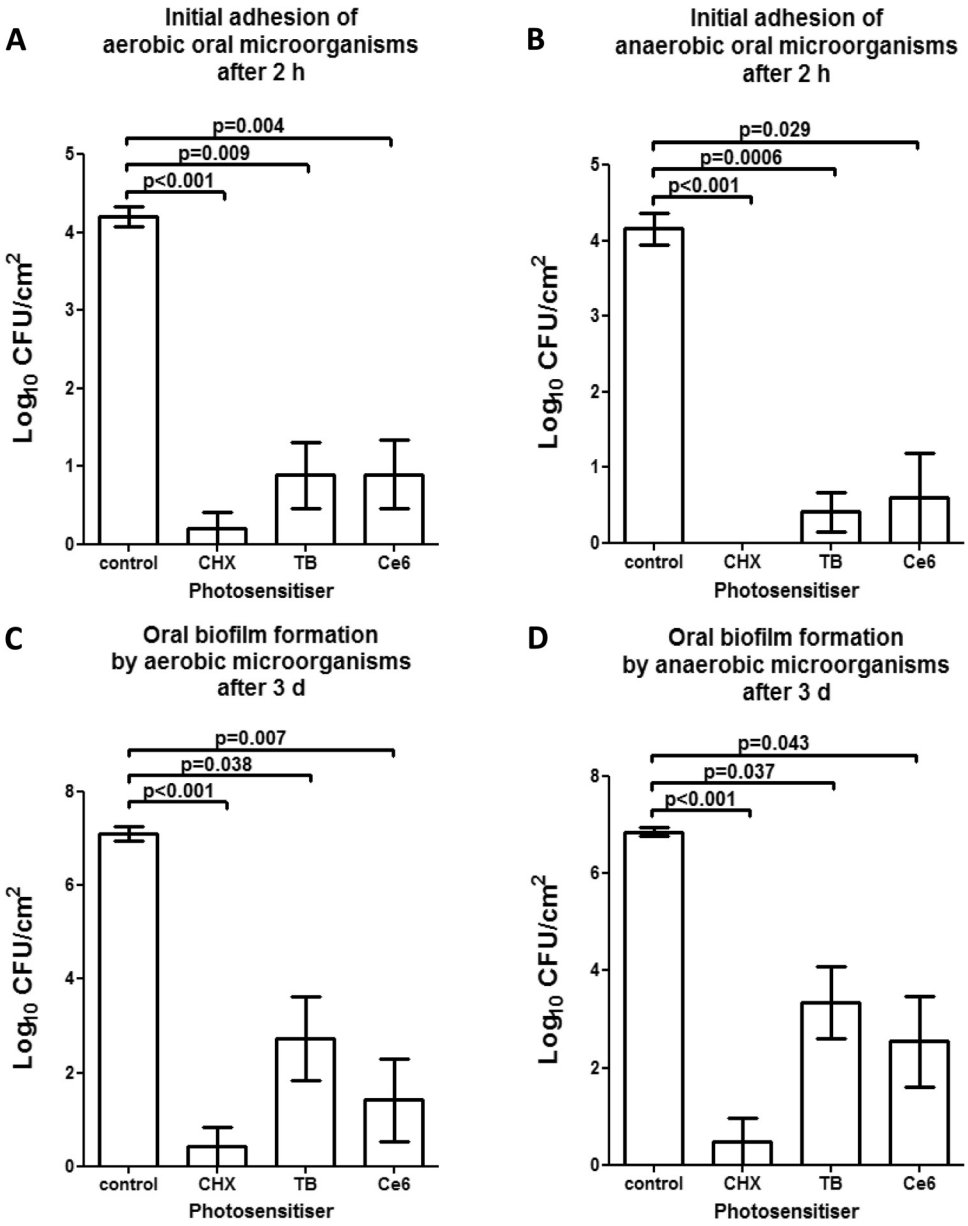

FIG 3 Graphs of the numbers of CFU, demonstrating the photodynamic efficiency against aerobic and anaerobic oral microorganisms during initial adhesion (A and B) and biofilm formation (C and D), respectively. Toluidine blue (TB) and chlorin e6 (Ce6) served as photosensitizers. An untreated negative control and a chlorhexidine-treated (CHX) positive control were also tested after 2 h or 3 days, respectively. The CFU are presented on a $\log_{10}$ scale per square centimeter ($\log_{10}$/cm^2). The *P* values (*t* test) of the significantly different data are marked on the graphs.

croorganism (aerobic/anaerobic). An analysis of variance (ANOVA) was conducted to analyze the differences in vitality results for the APDT-treated biofilms and the controls. *P* values were adjusted by using the method of Scheffé. For each examined group (control, CHX, TB, and Ce6), the continuous-response variable was displayed as a boxplot of the detected viable oral microorganisms and separately as a boxplot of biofilm age (initial/mature). All calculations were done with the statistical software STATA 13.1.

RESULTS

APDT significantly decreased the viable counts of oral microorganisms during initial adhesion. Figure 3A and B show the high eradication rates of initially adherent oral aerobic (Fig. 3A) and anaerobic (Fig. 3B) microorganisms after the application of APDT using VIS + wIRA in the presence of TB and Ce6, plus the untreated negative and positive (CHX) controls. APDT induced a substantial reduction of more than 99.99% in the viable bacterial count after 2 h of initial microbial adhesion *in situ*, independent of the photosensitizer.

Regarding the initially adherent oral aerobic microorganisms in particular (Fig. 3A), the untreated control revealed a $\log_{10}$ CFU value of 4.2 ± 0.3 (median, 4.15), while the CFU counts of the CHX-treated positive control were 0.2 ± 0.5 $\log_{10}$. The application of APDT using TB yielded a significant decrease ($P = 0.009$) of 3.8 CFU (mean, 0.88 ± 1; median, 0.62) on a $\log_{10}$ scale, while

Ce6-mediated APDT also induced a significant reduction ($P = 0.004$) of 3.7 $\log_{10}$ CFU (mean, 0.89 ± 1; median, 0.61).

APDT proved to be highly effective against initially adherent oral anaerobic microorganisms (Fig. 3B). Compared with the untreated negative control exhibiting CFU values of 4.15 ± 0.5 (median, 4.13), APDT using TB (mean, 0.4 ± 0.63) significantly ($P = 0.0006$) reduced the CFU counts by 3.7 $\log_{10}$. Similarly, APDT using Ce6 (mean, 0.59 ± 1.44) significantly reduced ($P = 0.029$) the numbers of viable anaerobic microorganisms by 3.7 $\log_{10}$ compared with the untreated control. No cultivable anaerobic bacteria were detected after treatment with CHX (positive control).

APDT significantly reduced the number of cultivable microorganisms within mature oral biofilms. Figure 3C and D demonstrates the elevated elimination rates of aerobic (Fig. 3C) and anaerobic (Fig. 3D) microorganisms within the oral biofilm after treatment with VIS + wIRA-derived APDT in the presence of TB and Ce6 as well as of the untreated negative and positive (CHX) controls. Upon use of APDT combined with either TB or Ce6, the viable counts of oral biofilm microorganisms were significantly suppressed, corresponding to a minimum reduction of 99.9% in the 3-day-old biofilm.

As for the aerobic biofilm bacteria, TB-mediated APDT (mean, 2.73 ± 2.19; median, 3.47) yielded a significant CFU decline ($P = 0.038$) of 4.37 $\log_{10}$ compared with the untreated negative control (mean, 7.1 ± 0.36; median, 7.08). In the same manner, application of Ce6-mediated APDT (mean, 1.41 ± 2.18) significantly lowered ($P = 0.007$) the CFU counts by 5.7 $\log_{10}$ compared to the negative control, i.e., it exhibited effectiveness similar to that of CHX (mean, 0.42 ± 1.03).

The high-level of antimicrobial activity for APDT was also confirmed for the anaerobic biofilm microorganisms. The untreated 3-day oral biofilms contained on average 6.87 ± 0.16 $\log_{10}$ (median, 6.87) of viable anaerobic bacteria, which were substantially diminished by 3.53 $\log_{10}$ ($P = 0.037$) and 4.33 $\log_{10}$ ($P = 0.043$) after the application of APDT using either TB (mean, 3.34 ± 1.81; median, 3.69), or Ce6 (mean, 2.54 ± 2.28, median, 2.53), respectively. The CHX-treated 3-day biofilms (mean, 0.48 ± 1.19) showed a reduction in CFU ($P > 0.1$) comparable to that seen in the APDT-treated groups.

Live/dead assays revealed surprisingly high bactericidal activity for APDT against oral biofilms. The quantitative results of the remaining vital bacteria detected by the live/dead assay during initial adhesion (2 h) and oral biofilm formation (3 days) after APDT using VIS + wIRA and two different photosensitizers (TB, Ce6) are depicted in Fig. 4 in the form of boxplots.

Without any treatment, 74.47% of the BES (negative control) was coated with viable, initially adherent bacteria (Fig. 4A). Statistical analysis revealed substantial differences ($P < 0.001$) in the percentages of vital bacteria between biofilms receiving TB-mediated APDT (20.7%) or Ce6-mediated APDT (12.12%) and the untreated control. In fact, in the presence of Ce6, significantly more microorganisms were killed ($P = 0.001$) than with TB. A total of 17.27% of the bacteria remained vital after treatment with CHX, corresponding to the amounts yielded with APDT.

APDT using VIS + wIRA and either TB or Ce6 demonstrated significantly reduced vitality percentages ($P < 0.001$) of 17.75% and 10.38%, respectively, compared with the untreated mature biofilms (82.12%) (Fig. 4B). Ce6-mediated APDT showed higher efficacy in eliminating biofilms ($P < 0.001$) than TB-aided APDT

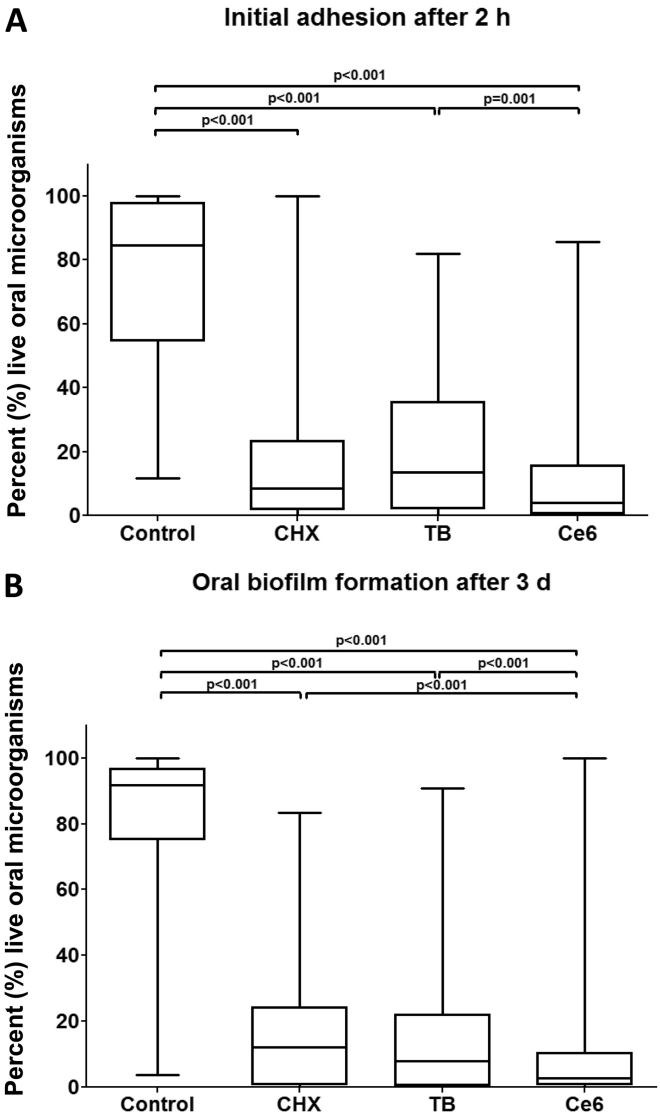

FIG 4 Boxplots depicting percentages of the live oral microorganisms as detected by live/dead staining after the application of photodynamic therapy during initial adhesion (A) and biofilm formation (B), respectively. Toluidine blue (TB) and chlorin e6 (Ce6) served as photosensitizers. An untreated negative control and a chlorhexidine-treated (CHX) positive control were also examined after 2 h or 3 days, respectively. The internal line represents the median; whiskers indicate minimum and maximum. The *P* values (ANOVA, Scheffé adjustment) of the significantly different data are provided.

and the CHX-treated controls (16.43%). The percentages presented above are all median values.

Figure 5 shows representative cross-sectional CLSM images of live/dead stained initial oral biofilms (2 h) after the application of APDT using VIS + wIRA and TB or Ce6 as photosensitizers.

Regarding the untreated control (Fig. 5A), a dense accumulation of viable (green) bacteria on BES was detected. Interestingly, initial oral biofilms exposed solely to either TB (Fig. 5E) or Ce6 (Fig. 5F) in the absence of VIS + wIRA also retained their viability and biomass volume. Very few cells were nonviable (red). The majority of coccoid or filamentous microorganisms, mainly streptococci, exhibited diverse arrangements of single cocci, mono- or multistratified chains, and three-dimensional bacterial aggregates

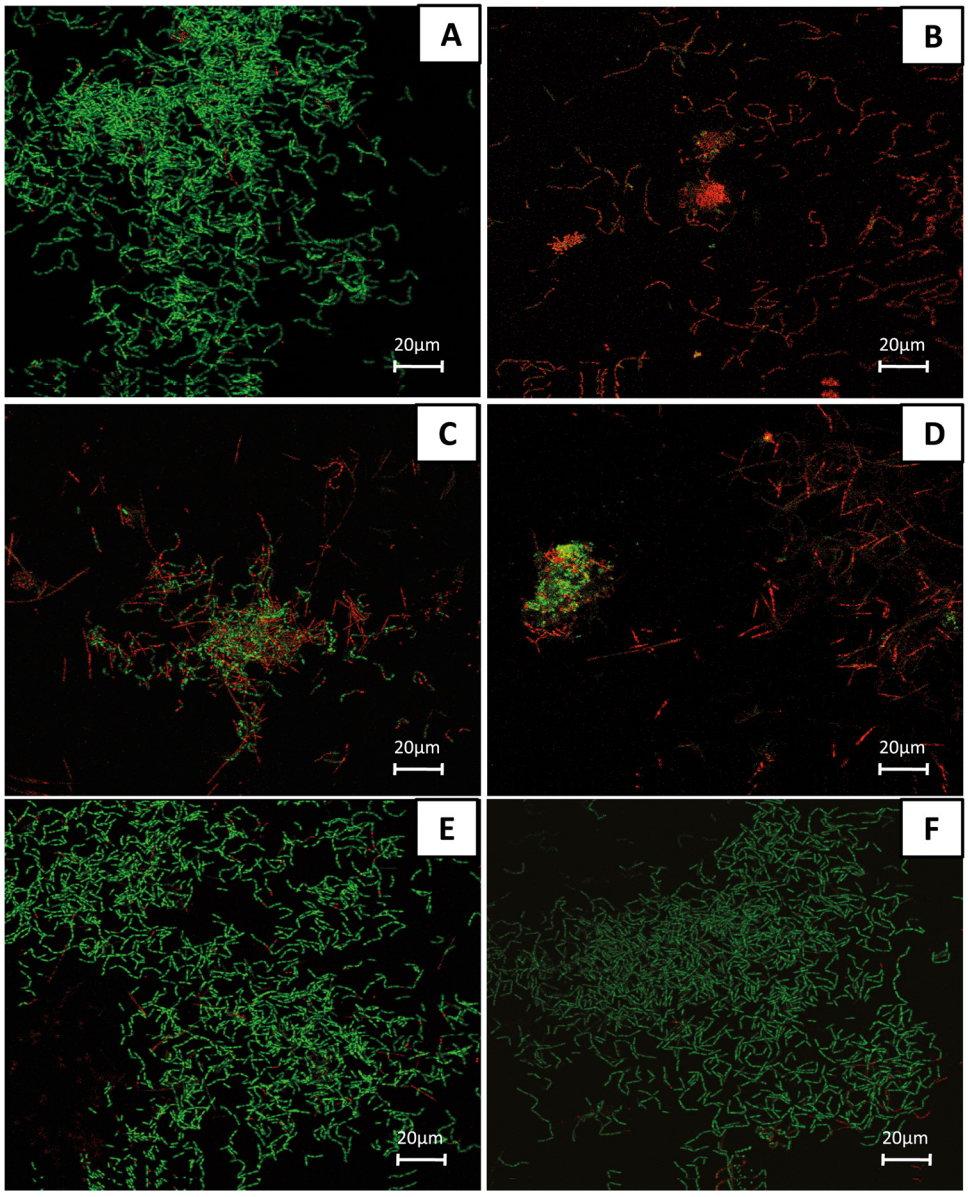

FIG 5 Confocal laser scanning microscopic (CLSM) images depicting the photodynamic effect on initial microbial adhesion (2 h) after live/dead staining. The panels illustrate the live (green) and dead (red) microbial populations of the untreated negative control (A), the chlorhexidine-treated (CHX) positive control (B), and the toluidine blue (TB)-treated (C) and chlorin e6 (Ce6)-treated (D) groups in the presence of VIS + wIRA and the TB-treated (E) and Ce6-treated (F) groups in the absence of VIS + wIRA. Each panel demonstrates maximum projections of the imaged area on the bovine enamel surface. Bars, 20 μm.

varying in size. In contrast to the negative controls, the spatial structure of initial oral biofilms treated with VIS + wIRA using either TB (Fig. 5C) or Ce6 (Fig. 5D) was markedly distinct. In fact, the APDT-treated biofilms were less confluent and irregularly distributed, probably due to detachment of the nonviable microorganisms. Apart from cell-substratum separation, APDT caused cell death of the majority of the attached bacteria, which was also seen for the CHX-treated biofilms (Fig. 5B).

CLSM images showed high permeativity of TB and Ce6 within APDT-treated oral biofilms. Figure 6 depicts representative cross-sectional CLSM images of live/dead stained mature oral biofilms (3 days) after the application of APDT using VIS + wIRA and the photosensitizer TB or Ce6.

Inspection of the untreated control biofilms revealed numerous, densely organized viable (green) microorganisms (Fig. 6A) in various configurations. Very few homeostasis-associated nonviable cells (red) were also present. On the other hand, treatment of mature oral biofilms with CHX (positive controls) induced a massive loss in cell viability, as depicted by the numerous red-stained bacteria (Fig. 6B). However, sparse green areas indicated the existence of persistent cells within the biofilms. The biofilms treated with APDT and either TB (Fig. 6C) or Ce6 (Fig. 6D) included a vast amount of dead microorganisms without any detectable alteration of the average biofilm thickness. Interestingly, visual observation of the Z-section CLSM galleries (Fig. 6C and D) reflected the different degree of biofilm permeability, dependent on the

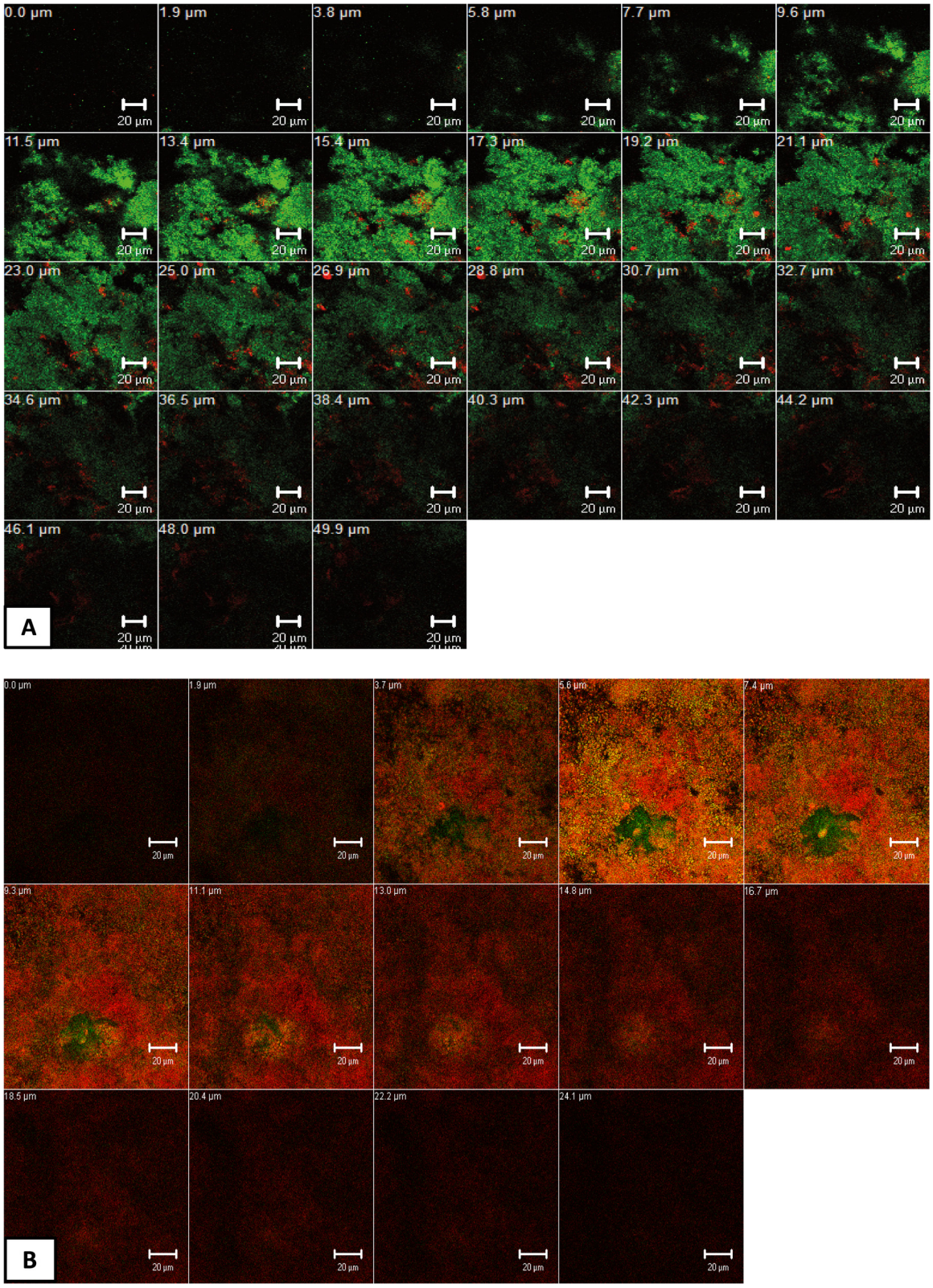

FIG 6 Z-section galleries of representative confocal laser scanning microscopic (CLSM) images depicting the photodynamic effect on oral biofilm formation (3 days) after live/dead staining. The panels illustrate the live (green) and dead (red) microbial populations of the untreated negative control (A), the chlorhexidine-treated (CHX) positive control (B), and APDT-treated groups in the presence of either toluidine blue (TB) (C) or chlorin e6 (Ce6) (D). The multiple Z sections in panels A to D were generated by vertical sectioning in 0.5-μm (A) or 2.0-μm (B to D) intervals through the sample above the bovine enamel surface, respectively. Bars, 20 μm.

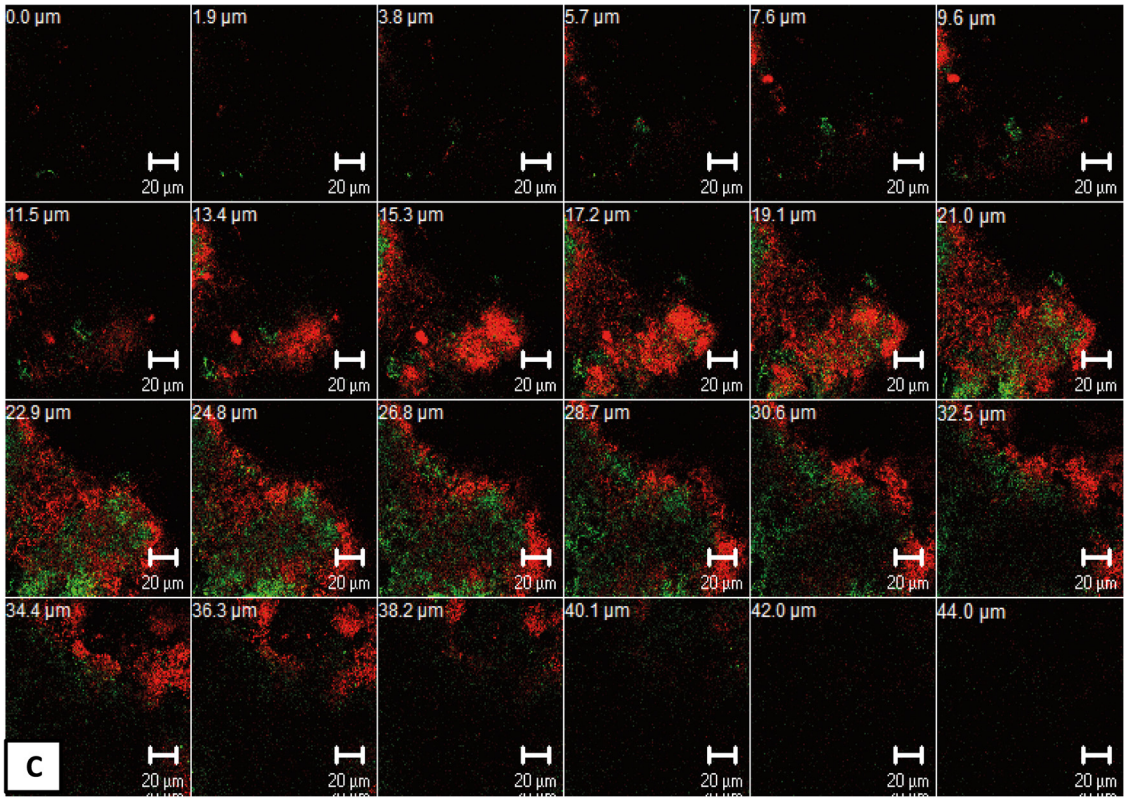

FIG 6 continued

photosensitizer. In particular, the oral biofilm was more permeable to Ce6 than for TB, as highlighted by the increasing amount of viable microorganisms in the deeper biofilm layers after exposure to TB-mediated APDT.

DISCUSSION

The present report establishes for the first time a potent target-specific antimicrobial photodynamic approach using VIS + wIRA with two different photosensitizing agents (TB and Ce6) to treat *in situ*-formed initial and mature oral biofilms. The innovation of this study is the assessment of VIS + wIRA as a light source for APDT. Technically, VIS + wIRA is a broad-band heat radiation generated by a halogen lamp with a continuous spectrum of unpolarized light emission within the range of 570 to 1,400 nm (17). After the radiation passes through a water filter, which absorbs or decreases harmful infrared B and C radiation, the remaining infrared A can deeply penetrate the target tissues with a low thermal load (28). To date, therapy with VIS + wIRA has been mainly utilized in dermatology for the treatment of superficial skin tumors, wound healing, and pain alleviation (29, 30). The extension of its application in the microbiological field, i.e., for postoperative infection defense, or photoinactivation of oral pathogenic microorganisms, can be attributed to the advanced antimicrobial properties of VIS + wIRA (20).

In order to accentuate the amount of the emitted water-filtered infrared A (wIRA; in the range of 780 to 1,400 nm), a visible light (VIS) source with an accessory orange filter (within the range of 570 to 780 nm) can be utilized (31). As a result, amplified energy and, thus, greater amounts of oxygen due to increased metabolic rates are transmitted to deeper tissue layers, avoiding thermal stress on tissue surfaces (32). Beside its nonthermal effects, wIRA has an advantageous stimulatory impact on cytochrome *c* oxidase, a regulatory enzyme with absorption maxima at 620, 680, 760, and 825 nm (33, 34). Within cytochrome *c* oxidase, VIS serves as an electron trigger, while wIRA activates an internal electron transfer, leading to increased production of ATP in the initial phase of several cellular signaling cascades (35). From a physiological point of view, the use of high spectral irradiance such as VIS + wIRA allows optimal photoactivation of cytochrome *c* oxidase and was therefore chosen as the main APDT light source in our study. The application of wIRA alone would not be effective, as the tested photosensitizers can be excited only within the range of VIS (31, 32). The favorable outcomes of the application of VIS + wIRA compared with VIS alone were also highlighted in previous reports (16, 31).

The main antimicrobial traits of VIS + wIRA are demonstrated directly by improving both cellular energy and oxygen supply, thereby increasing the production of reactive oxygen species (ROS) and singlet oxygen ($^1O_2$) (type I and II reactions) (32). Moreover, in contrast with other conventional APDT light sources (laser and nonlaser radiators), VIS + wIRA has the advantage of promoting photobactericidal effects during APDT in an indirect way (31). In particular, VIS + wIRA can activate immunoregulatory mechanisms to prevent inflammation and induce capillary vasodilation (18). As a result, increased blood circulation enables active distribution of antibiotics to the infected sites and the elimination of bacterial endotoxins (36, 37). Due to the deep tissue penetration of VIS + wIRA (up to 3 cm), the bacterial growth of deep-seated microorganisms is inhibited, especially at subcutaneous locations with low (9 to 39%) antibiotic diffusion rates (16). Interestingly, VIS + wIRA triggers the production of protective proteins such as ferritin, which avert further cell damage (38). Radiators emitting VIS + wIRA were found to be less painful than LED devices and extremely safe when applied with different treatment doses of up to 30 min (23, 38, 39). However, the moderate treatment duration of 5 min applied in our report proved to be effective and more realistic for everyday dental clinical practice.

The use of bovine enamel slabs simulates a representative substratum model for the study of bacterial adherence to tooth surfaces because they share physicochemical features with adamantine human dental tissues. Large numbers of reproducible planar bovine enamel surfaces can be easily obtained. The use of artificial tooth substrata was omitted because the composition of their biofilms can show discrepancies with those growing on natural tooth surfaces (40). Regarding CLSM imaging, enamel autofluorescence did not interfere with obtaining fluorescence signals from the *in situ* oral biofilms, despite the contradictory findings in a previous report (41).

CFU quantification showed that an energy density of 200 mW cm^{-2} with a photosensitizer (TB or Ce6) concentration of 100 μg ml^{-1}, the bacterial cell counts of 2-h- and 3-day-old oral biofilms showed a logarithmic reduction up to factors of 3.8 and 5.7, respectively. This is in agreement with the outcomes of a previous study from our group on APDT using VIS + wIRA, in which successful outcomes were achieved against initially (2 h) *in situ*-adherent bacteria at even lower TB concentrations of up to 10 μg ml^{-2} (20). Similarly, encouraging APDT-induced CFU reduction was observed in numerous *in vitro* studies with various other light sources and photosensitizers (42–45). Regarding oral pathogenic bacteria in particular, the posttreatment decrease in viable bacterial counts has also been confirmed in several *in vitro* studies to date (28, 46–49). For instance, Pfitzner et al., using diode laser-mediated APDT and the Ce6 and BLC 1010 photosensitizers at concentrations of 10 μM, were able to thoroughly inactivate oral anaerobic microorganisms, i.e., *Porphyromonas gingivalis*, *Fusobacterium nucleatum*, and *Capnocytophaga gingivalis* (46). Furthermore, Zanin et al. showed that APDT with an LED energy density of 85.7 J cm^{-2} in the presence of TB (0.1 mg ml^{-1}) significantly reduced the cell count of *Streptococcus mutans* biofilms from 7.45×10^7 to 3.75×10^6 CFU mg^{-1} (47). However, the estimation that about 50% of the oral species are not cultivable is an inherent limitation of the culture method (50).

Use of the live/dead viability assay not only supplemented the CFU quantification results but also enabled nondestructive visualization of the APDT-treated oral biofilms, thereby reflecting the diffusion rates of the tested photosensitizers into the biofilms. The number of vital microorganisms declined significantly after APDT with TB or Ce6, confirming the outcomes of CFU quantification. This suggests that a posttreatment decrease in green fluorescence signals can be proportionally attributed to photosensitizer incorporation within the bacterial cells rather than to competitive inhibition, namely, the interference of TB or Ce6 with the binding of the live/dead dyes to intracellular targets. A similar tendency was also shown in several *in vitro* reports concerning the application of various APDT methods and photosensitizers to bacteria (51–53). Nevertheless, Pfitzner et al. interpreted their contradictory results as resulting from the presence of fluorescent photosensitizers, which possibly make the measured number of nonvital microorganisms stained with SYTO 9–PI inaccurate

(46). Interestingly, oral biofilms treated solely with either TB or Ce6 in the absence of VIS + wIRA remained viable. Similarly, the application of radiation without the photosensitizing agent proved to be ineffective in terms of bacterial photoinactivation in previous studies (54–56). This highlights the importance of the combined use of the photosensitizers with the appropriate APDT light source.

TB, a cationic phenothiazinium-based stain, contains potent monomer and dimer photodestructive species, which directly attach to and dismantle the exterior layers of bacterial cells (57). With regard to Gram-negative bacteria in particular, the photodynamic molecules bind to specific negatively charged lipopolysaccharide (LPS) sites on the outer cell membranes. Concerning Gram-positive species, receptors localized to teichuronic acid (TUA) recognize dye aggregates on the external peptidoglycan surfaces (58, 59). After excitation, the accumulated TB invades the bacterial cytoplasm via membrane stress, thereby destroying photolabile proteins and lipids or even inducing modest DNA degradation (60). Compared to the phenothiazinium salt methylene blue (MB), TB induces greater phototoxicity (61). In fact, its higher intracellular concentration is attributed to the increased solubility of TB in the hydrophobic bacterial membrane (58). On the other hand, the hydrophilic TB exhibits limited diffusion into the double-layered phospholipid membrane of the mammalian cells, resulting in low cytocidal effects on host cells, as highlighted in several previous studies (62, 63). This is an encouraging fact for the future clinical application of this photosensitizer (64).

Indeed, the photobactericidal effectiveness of TB was confirmed in our report by the massive reduction (more than 99.99%) in the amount of viable aerobic and anaerobic bacterial counts after application of TB-mediated VIS + wIRA. Nevertheless, the detailed assessment of CLSM images of live/dead stained microorganisms revealed limited intrabiofilm dye permeability and therefore a lower bactericidal performance for TB than Ce6. This can be attributed to LPS-associated alterations on the surfaces of different anaerobic Gram-negative bacteria, mostly situated within the deeper layers of the biofilm (65). As a result, the adsorption of TB to LPS or other bacterial membrane biopolymers was presumed to be inhibited, since the dye's dimerization ability was negatively affected (57). Furthermore, TB probably failed to intercalate into extracellular DNA within the polysaccharide matrix, leading to incomplete diffusion of the photosensitizer to reach microorganisms within the deeper layers of the biofilm (51).

In order to compensate for potential photobleaching of TB under the influence of microorganisms, the photosensitizer chlorin e6 (Ce6; $C_{34}H_{36}N_4O_6$) was also tested (66). Ce6 is a chlorophyll *a*-based second-generation photosensitizing agent, which is derived from the green seawater alga *Chlorella* (*Chlorella ellipsoidea*) (67). Except for the fractional saturation of a pyrrole ring, its structural resemblance to porphyrins is responsible for the varying, pH-dependent charge of the molecule (68). As a result, the partition coefficient *P* and thereby its lipophilicity increase with declining pH values, leading to a higher Ce6 uptake by nonspecific lipoprotein targets on the bacterial membrane, especially in the presence of infrared radiation (69). The long-lasting photoexcited triplet state of Ce6 can also be considered a favorable photophysical feature of this plant-derived photosensitizer (68, 70). Interestingly, Ce6 also showed affinity for human serum albumin and low-density lipoproteins (LDL) (71). In terms of cytotoxicity, Ce6 alone has no significant toxic effects on host cells (72). Only in combination with locally administered photodynamic irradiation does Ce6 exhibit enhanced tumor-phototoxic properties, as it selectively accumulates in various intracellular targets of cancer cells (73). Other advantages of Ce6 include low-cost preparation, uncomplicated and rapid synthesis, and complete adsorption within bacterial target cells (67).

Ce6, carrying three carboxylic groups, showed a highly photosensitizing effect in this study. This is the reason that this molecule was chosen, as it allowed indirect comparison of the phototoxic potential of the carboxylic group number compared to the dicarboxylic porphyrins (71). Ce6 actually outperformed TB in terms of its photodestructive effect against live/dead-stained initial and mature dental plaque biofilms. As depicted in the CLSM images, Ce6 succeeded in deeply permeating the thicker 3-day-old oral biofilm. A plausible explanation for this phenomenon is the increase in the more acidic pH-activated Ce6-binding sites on the hydrophobic bacterial surfaces in the presence of pH values lower than 5.0 within the biofilms (5, 71). The latter are usually induced by acid formation via the glycolytic pathway of streptococcal carbohydrate metabolism (5). Furthermore, favorable alterations in cellular protein synthesis in the context of acid tolerance response (ATR) could promote intracellular adsorption of Ce6 (74). The superior photoactive efficiency of Ce6, although not statistically significant, was only partially supported by the CFU quantification of anaerobic microorganisms. This could imply the existence of a process of long-term inherent biofilm recovery which is not depicted by the live/dead viability assay and which is reflected solely by immediate bacterial cell death.

Another factor that determines the effectiveness of APDT is the preillumination exposure time of the photosensitizer (58). This implies that various chemically different photosensitizing agents need some time to reach the intracellular target locations of bacteria through translocation mechanisms, mainly diffusion or endocytosis (75). We therefore pre-exposed the biofilms to TB or Ce6 for 2 min in the dark in order to enable a better distribution of photosensitizer within the bacterial cells. It was shown that photosensitizer adsorption initially takes place in hydrophobic regions of the cytoplasmic membrane and later becomes more evident at other adjacent sites (28).

In conclusion, antimicrobial photoinactivation using VIS + wIRA in the presence of different photosensitizing agents (TB and Ce6) proved highly effective at treating *in situ*-formed initial and mature oral biofilms. Therefore, APDT could be added to the reservoir of novel antimicrobial strategies to supplement conventional resistance-evoking oral pharmaceuticals. In the future, the application of similar methodological approaches should aim to investigate the effectiveness of novel photosensitizing agents in combination with VIS + wIRA, as well as to study the impact of APDT by VIS + wIRA on dental patients suffering from periodontitis or peri-implantitis.

ACKNOWLEDGMENTS

Bettina Spitzmüller is acknowledged for skillful technical laboratory assistance during the live/dead assay.

This study was supported by the Swiss Dr. Braun Science Foundation and in part by the German Research Foundation (DFG, AL 1179/1-1).

REFERENCES

1. **Madianos PN, Bobetsis YA, Kinane DF.** 2005. Generation of inflammatory stimuli: how bacteria set up inflammatory responses in the gingiva. J.

Clin. Periodontol. **32**(Suppl 6):S57–S71. http://dx.doi.org/10.1111/j.1600-051X.2005.00821.x.
2. **Filoche S, Wong L, Sissons CH.** 2010. Oral biofilms: emerging concepts in microbial ecology. J. Dent. Res. **89:**8–18. http://dx.doi.org/10.1177/0022034509351812.
3. **Kolenbrander PE, Palmer RJ, Jr, Periasamy S, Jakubovics NS.** 2010. Oral multispecies biofilm development and the key role of cell-cell distance. Nat. Rev. Microbiol. **8:**471–480. http://dx.doi.org/10.1038/nrmicro2381.
4. **McBain AJ, Bartolo RG, Catrenich CE, Charbonneau D, Ledder RG, Gilbert P.** 2003. Effects of a chlorhexidine gluconate-containing mouthwash on the vitality and antimicrobial susceptibility of in vitro oral bacterial ecosystems. Appl. Environ. Microbiol. **69:**4770–4776. http://dx.doi.org/10.1128/AEM.69.8.4770-4776.2003.
5. **Welin-Neilands J, Svensater G.** 2007. Acid tolerance of biofilm cells of Streptococcus mutans. Appl. Environ. Microbiol. **73:**5633–5638. http://dx.doi.org/10.1128/AEM.01049-07.
6. **Adriaens PA, Adriaens LM.** 2004. Effects of nonsurgical periodontal therapy on hard and soft tissues. Periodontol. 2000 **36:**121–145. http://dx.doi.org/10.1111/j.1600-0757.2004.03676.x.
7. **Moan J, Peng Q.** 2003. An outline of the hundred-year history of PDT. Anticancer Res. **23:**3591–3600.
8. **Takasaki AA, Aoki A, Mizutani K, Schwarz F, Sculean A, Wang CY, Koshy G, Romanos G, Ishikawa I, Izumi Y.** 2009. Application of antimicrobial photodynamic therapy in periodontal and peri-implant diseases. Periodontol. 2000 **51:**109–140. http://dx.doi.org/10.1111/j.1600-0757.2009.00302.x.
9. **Cieplik F, Spath A, Regensburger J, Gollmer A, Tabenski L, Hiller KA, Baumler W, Maisch T, Schmalz G.** 2013. Photodynamic biofilm inactivation by SAPYR—an exclusive singlet oxygen photosensitizer. Free Radic. Biol. Med. **65:**477–487. http://dx.doi.org/10.1016/j.freeradbiomed.2013.07.031.
10. **Maisch T, Szeimies RM, Jori G, Abels C.** 2004. Antibacterial photodynamic therapy in dermatology. Photochem. Photobiol. Sci. **3:**907–917. http://dx.doi.org/10.1039/b407622b.
11. **Konopka K, Goslinski T.** 2007. Photodynamic therapy in dentistry. J. Dent. Res. **86:**694–707. http://dx.doi.org/10.1177/154405910708600803.
12. **Freinbichler W, Colivicchi MA, Stefanini C, Bianchi L, Ballini C, Misini B, Weinberger P, Linert W, Vareslija D, Tipton KF, Della Corte L.** 2011. Highly reactive oxygen species: detection, formation, and possible functions. Cell. Mol. Life Sci. **68:**2067–2079. http://dx.doi.org/10.1007/s00018-011-0682-x.
13. **Nagata JY, Hioka N, Kimura E, Batistela VR, Terada RS, Graciano AX, Baesso ML, Hayacibara MF.** 2012. Antibacterial photodynamic therapy for dental caries: evaluation of the photosensitizers used and light source properties. Photodiagn. Photodyn. Ther. **9:**122–131. http://dx.doi.org/10.1016/j.pdpdt.2011.11.006.
14. **Wilson BC, Patterson MS.** 2008. The physics, biophysics and technology of photodynamic therapy. Phys. Med. Biol. **53:**R61–R109. http://dx.doi.org/10.1088/0031-9155/53/9/R01.
15. **Daeschlein G, Alborova J, Patzelt A, Kramer A, Lademann J.** 2012. Kinetics of physiological skin flora in a suction blister wound model on healthy subjects after treatment with water-filtered infrared-A radiation. Skin Pharmacol. Physiol. **25:**73–77. http://dx.doi.org/10.1159/000332753.
16. **Hartel M, Hoffmann G, Wente MN, Martignoni ME, Buchler MW, Friess H.** 2006. Randomized clinical trial of the influence of local water-filtered infrared A irradiation on wound healing after abdominal surgery. Br. J. Surg. **93:**952–960. http://dx.doi.org/10.1002/bjs.5429.
17. **Jung T, Grune T.** 2012. Experimental basis for discriminating between thermal and athermal effects of water-filtered infrared A irradiation. Ann. N. Y. Acad. Sci. **1259:**33–38. http://dx.doi.org/10.1111/j.1749-6632.2012.06581.x.
18. **Kunzli BM, Liebl F, Nuhn P, Schuster T, Friess H, Hartel M.** 2013. Impact of preoperative local water-filtered infrared A irradiation on postoperative wound healing: a randomized patient- and observer-blinded controlled clinical trial. Ann. Surg. **258:**887–894. http://dx.doi.org/10.1097/SLA.0000000000000235.
19. **von Felbert V, Schumann H, Mercer JB, Strasser W, Daeschlein G, Hoffmann G.** 2008. Therapy of chronic wounds with water-filtered infrared-A (wIRA). GMS Krankenhhyg. Interdiszip. **2:**Doc52.
20. **Al-Ahmad A, Tennert C, Karygianni L, Wrbas KT, Hellwig E, Altenburger MJ.** 2013. Antimicrobial photodynamic therapy using visible light plus water-filtered infrared-A (wIRA). J. Med. Microbiol. **62:**467–473. http://dx.doi.org/10.1099/jmm.0.048843-0.
21. **Karygianni L, Follo M, Hellwig E, Burghardt D, Wolkewitz M, Anderson A, Al-Ahmad A.** 2012. Microscope-based imaging platform for large-scale analysis of oral biofilms. Appl. Environ. Microbiol. **78:**8703–8711. http://dx.doi.org/10.1128/AEM.02416-12.
22. **Al-Ahmad A, Follo M, Selzer AC, Hellwig E, Hannig M, Hannig C.** 2009. Bacterial colonization of enamel in situ investigated using fluorescence in situ hybridization. J. Med. Microbiol. **58:**1359–1366. http://dx.doi.org/10.1099/jmm.0.011213-0.
23. **Piazena H, Kelleher DK.** 2010. Effects of infrared-A irradiation on skin: discrepancies in published data highlight the need for an exact consideration of physical and photobiological laws and appropriate experimental settings. Photochem. Photobiol. **86:**687–705. http://dx.doi.org/10.1111/j.1751-1097.2010.00729.x.
24. **Nogueira AC, Graciano AX, Nagata JY, Fujimaki M, Terada RS, Bento AC, Astrath NG, Baesso ML.** 2013. Photosensitizer and light diffusion through dentin in photodynamic therapy. J. Biomed. Opt. **18:**55004. http://dx.doi.org/10.1117/1.JBO.18.5.055004.
25. **Paul S, Heng PW, Chan LW.** 2013. Optimization in solvent selection for chlorin e6 in photodynamic therapy. J. Fluoresc. **23:**283–291. http://dx.doi.org/10.1007/s10895-012-1146-x.
26. **Tawakoli PN, Al-Ahmad A, Hoth-Hannig W, Hannig M, Hannig C.** 2013. Comparison of different live/dead stainings for detection and quantification of adherent microorganisms in the initial oral biofilm. Clin. Oral Invest. **17:**841–850. http://dx.doi.org/10.1007/s00784-012-0792-3.
27. **Al-Ahmad A, Wunder A, Auschill TM, Follo M, Braun G, Hellwig E, Arweiler NB.** 2007. The in vivo dynamics of Streptococcus spp., Actinomyces naeslundii, Fusobacterium nucleatum and Veillonella spp. in dental plaque biofilm as analysed by five-colour multiplex fluorescence in situ hybridization. J. Med. Microbiol. **56:**681–687. http://dx.doi.org/10.1099/jmm.0.47094-0.
28. **Rolim JP, de-Melo MA, Guedes SF, Albuquerque-Filho FB, de Souza JR, Nogueira NA, Zanin IC, Rodrigues LK.** 2012. The antimicrobial activity of photodynamic therapy against Streptococcus mutans using different photosensitizers. J. Photochem. Photobiol. B **106:**40–46. http://dx.doi.org/10.1016/j.jphotobiol.2011.10.001.
29. **Hurlimann AF, Hanggi G, Panizzon RG.** 1998. Photodynamic therapy of superficial basal cell carcinomas using topical 5-aminolevulinic acid in a nanocolloid lotion. Dermatology **197:**248–254. http://dx.doi.org/10.1159/000018006.
30. **Akca O, Melischek M, Scheck T, Hellwagner K, Arkilic CF, Kurz A, Kapral S, Heinz T, Lackner FX, Sessler DI.** 1999. Postoperative pain and subcutaneous oxygen tension. Lancet **354:**41–42. http://dx.doi.org/10.1016/S0140-6736(99)00874-0.
31. **Schumann H, Calow T, Weckesser S, Muller ML, Hoffmann G.** 2011. Water-filtered infrared A for the treatment of chronic venous stasis ulcers of the lower legs at home: a randomized controlled blinded study. Br. J. Dermatol. **165:**541–551. http://dx.doi.org/10.1111/j.1365-2133.2011.10410.x.
32. **von Felbert V, Hoffmann G, Hoff-Lesch S, Abuzahra F, Renn CN, Braathen LR, Merk HF.** 2010. Photodynamic therapy of multiple actinic keratoses: reduced pain through use of visible light plus water-filtered infrared A compared with light from light-emitting diodes. Br. J. Dermatol. **163:**607–615. http://dx.doi.org/10.1111/j.1365-2133.2010.09817.x.
33. **Karu TI.** 2010. Multiple roles of cytochrome c oxidase in mammalian cells under action of red and IR-A radiation. IUBMB Life. **62:**607–610. http://dx.doi.org/10.1002/iub.359.
34. **Karu TI, Pyatibrat LV, Kalendo GS.** 2001. Cell attachment to extracellular matrices is modulated by pulsed radiation at 820 nm and chemicals that modify the activity of enzymes in the plasma membrane. Lasers Surg. Med. **29:**274–281. http://dx.doi.org/10.1002/lsm.1119.
35. **Karu TI.** 2008. Mitochondrial signaling in mammalian cells activated by red and near-IR radiation. Photochem. Photobiol. **84:**1091–1099. http://dx.doi.org/10.1111/j.1751-1097.2008.00394.x.
36. **Rendell MS, Milliken BK, Finnegan MF, Finney DA, Healy JC.** 1997. The skin blood flow response in wound healing. Microvasc. Res. **53:**222–234. http://dx.doi.org/10.1006/mvre.1997.2008.
37. **Fuchs SM, Fluhr JW, Bankova L, Tittelbach J, Hoffmann G, Elsner P.** 2004. Photodynamic therapy (PDT) and waterfiltered infrared A (wIRA)

in patients with recalcitrant common hand and foot warts. Ger. Med. Sci. **2:**Doc08.
38. **Jung T, Hohn A, Piazena H, Grune T.** 2010. Effects of water-filtered infrared A irradiation on human fibroblasts. Free Radic. Biol. Med. **48:**153–160. http://dx.doi.org/10.1016/j.freeradbiomed.2009.10.036.
39. **Giehl KA, Kriz M, Grahovac M, Ruzicka T, Berking C.** 2014. A controlled trial of photodynamic therapy of actinic keratosis comparing different red light sources. Eur. J. Dermatol. **24:**335–341. http://dx.doi.org/10.1684/ejd.2014.2364.
40. **Teles FR, Teles RP, Sachdeo A, Uzel NG, Song XQ, Torresyap G, Singh M, Papas A, Haffajee AD, Socransky SS.** 2012. Comparison of microbial changes in early redeveloping biofilms on natural teeth and dentures. J. Periodontol. **83:**1139–1148. http://dx.doi.org/10.1902/jop.2012.110506.
41. **Wood SR, Kirkham J, Marsh PD, Shore RC, Nattress B, Robinson C.** 2000. Architecture of intact natural human plaque biofilms studied by confocal laser scanning microscopy. J. Dent. Res. **79:**21–27. http://dx.doi.org/10.1177/00220345000790010201.
42. **Embleton ML, Nair SP, Heywood W, Menon DC, Cookson BD, Wilson M.** 2005. Development of a novel targeting system for lethal photosensitization of antibiotic-resistant strains of Staphylococcus aureus. Antimicrob. Agents Chemother. **49:**3690–3696. http://dx.doi.org/10.1128/AAC.49.9.3690-3696.2005.
43. **Tegos GP, Anbe M, Yang C, Demidova TN, Satti M, Mroz P, Janjua S, Gad F, Hamblin MR.** 2006. Protease-stable polycationic photosensitizer conjugates between polyethyleneimine and chlorin(e6) for broad-spectrum antimicrobial photoinactivation. Antimicrob. Agents Chemother. **50:**1402–1410. http://dx.doi.org/10.1128/AAC.50.4.1402-1410.2006.
44. **Tang HM, Hamblin MR, Yow CM.** 2007. A comparative in vitro photoinactivation study of clinical isolates of multidrug-resistant pathogens. J. Infect. Chemother. **13:**87–91. http://dx.doi.org/10.1007/s10156-006-0501-8.
45. **Ragas X, Dai T, Tegos GP, Agut M, Nonell S, Hamblin MR.** 2010. Photodynamic inactivation of Acinetobacter baumannii using phenothiazinium dyes: in vitro and in vivo studies. Lasers Surg. Med. **42:**384–390. http://dx.doi.org/10.1002/lsm.20922.
46. **Pfitzner A, Sigusch BW, Albrecht V, Glockmann E.** 2004. Killing of periodontopathogenic bacteria by photodynamic therapy. J. Periodontol. **75:**1343–1349. http://dx.doi.org/10.1902/jop.2004.75.10.1343.
47. **Zanin IC, Lobo MM, Rodrigues LK, Pimenta LA, Hofling JF, Goncalves RB.** 2006. Photosensitization of in vitro biofilms by toluidine blue O combined with a light-emitting diode. Eur. J. Oral Sci. **114:**64–69. http://dx.doi.org/10.1111/j.1600-0722.2006.00263.x.
48. **Eick S, Markauskaite G, Nietzsche S, Laugisch O, Salvi GE, Sculean A.** 2013. Effect of photoactivated disinfection with a light-emitting diode on bacterial species and biofilms associated with periodontitis and peri-implantitis. Photodiagn. Photodyn. Ther. **10:**156–167. http://dx.doi.org/10.1016/j.pdpdt.2012.12.001.
49. **Paschoal MA, Tonon CC, Spolidorio DM, Bagnato VS, Giusti JS, Santos-Pinto L.** 2013. Photodynamic potential of curcumin and blue LED against Streptococcus mutans in a planktonic culture. Photodiagn. Photodyn. Ther. **10:**313–319. http://dx.doi.org/10.1016/j.pdpdt.2013.02.002.
50. **Siqueira JF, Jr, Rocas IN.** 2005. Uncultivated phylotypes and newly named species associated with primary and persistent endodontic infections. J. Clin. Microbiol. **43:**3314–3319. http://dx.doi.org/10.1128/JCM.43.7.3314-3319.2005.
51. **Collins TL, Markus EA, Hassett DJ, Robinson JB.** 2010. The effect of a cationic porphyrin on Pseudomonas aeruginosa biofilms. Curr. Microbiol. **61:**411–416. http://dx.doi.org/10.1007/s00284-010-9629-y.
52. **Park JH, Moon YH, Bang IS, Kim YC, Kim SA, Ahn SG, Yoon JH.** 2010. Antimicrobial effect of photodynamic therapy using a highly pure chlorin e6. Lasers Med. Sci. **25:**705–710. http://dx.doi.org/10.1007/s10103-010-0781-1.
53. **Schneider M, Kirfel G, Berthold M, Frentzen M, Krause F, Braun A.** 2012. The impact of antimicrobial photodynamic therapy in an artificial biofilm model. Lasers Med. Sci. **27:**615–620. http://dx.doi.org/10.1007/s10103-011-0998-7.
54. **de Melo WDCMA, Lee AN, Perussi JR, Hamblin MR.** 2013. Electroporation enhances antimicrobial photodynamic therapy mediated by the hydrophobic photosensitizer, hypericin. Photodiagn. Photodyn. Ther. **10:**647–650. http://dx.doi.org/10.1016/j.pdpdt.2013.08.001.
55. **Sung N, Back S, Jung J, Kim KH, Kim JK, Lee JH, Ra Y, Yang HC, Lim C, Cho S, Kim K, Jheon S.** 2013. Inactivation of multidrug resistant (MDR)- and extensively drug resistant (XDR)-Mycobacterium tuberculosis by photodynamic therapy. Photodiagn. Photodyn. Ther. **10:**694–702. http://dx.doi.org/10.1016/j.pdpdt.2013.09.001.
56. **Tubby S, Wilson M, Wright JA, Zhang P, Nair SP.** 2013. Staphylococcus aureus small colony variants are susceptible to light activated antimicrobial agents. BMC Microbiol. **13:**201. http://dx.doi.org/10.1186/1471-2180-13-201.
57. **Usacheva MN, Teichert MC, Biel MA.** 2003. The role of the methylene blue and toluidine blue monomers and dimers in the photoinactivation of bacteria. J. Photochem. Photobiol. B **71:**87–98. http://dx.doi.org/10.1016/j.jphotobiol.2003.06.002.
58. **Usacheva MN, Teichert MC, Biel MA.** 2001. Comparison of the methylene blue and toluidine blue photobactericidal efficacy against gram-positive and gram-negative microorganisms. Lasers Surg. Med. **29:**165–173. http://dx.doi.org/10.1002/lsm.1105.
59. **Jori G, Fabris C, Soncin M, Ferro S, Coppellotti O, Dei D, Fantetti L, Chiti G, Roncucci G.** 2006. Photodynamic therapy in the treatment of microbial infections: basic principles and perspective applications. Lasers Surg. Med. **38:**468–481. http://dx.doi.org/10.1002/lsm.20361.
60. **Phoenix DA, Sayed Z, Hussain S, Harris F, Wainwright M.** 2003. The phototoxicity of phenothiazinium derivatives against Escherichia coli and Staphylococcus aureus. FEMS Immunol. Med. Microbiol. **39:**17–22. http://dx.doi.org/10.1016/S0928-8244(03)00173-1.
61. **Demidova TN, Hamblin MR.** 2005. Photodynamic inactivation of Bacillus spores, mediated by phenothiazinium dyes. Appl. Environ. Microbiol. **71:**6918–6925. http://dx.doi.org/10.1128/AEM.71.11.6918-6925.2005.
62. **Luan XL, Qin YL, Bi LJ, Hu CY, Zhang ZG, Lin J, Zhou CN.** 2009. Histological evaluation of the safety of toluidine blue-mediated photosensitization to periodontal tissues in mice. Lasers Med. Sci. **24:**162–166. http://dx.doi.org/10.1007/s10103-007-0513-3.
63. **Kashef N, Ravaei Sharif Abadi G, Djavid GE.** 2012. Photodynamic inactivation of primary human fibroblasts by methylene blue and toluidine blue O. Photodiagn. Photodyn. Ther. **9:**355–358. http://dx.doi.org/10.1016/j.pdpdt.2012.05.001.
64. **Tanaka M, Kinoshita M, Yoshihara Y, Shinomiya N, Seki S, Nemoto K, Hirayama T, Dai T, Huang L, Hamblin MR, Morimoto Y.** 2012. Optimal photosensitizers for photodynamic therapy of infections should kill bacteria but spare neutrophils. Photochem. Photobiol. **88:**227–232. http://dx.doi.org/10.1111/j.1751-1097.2011.01005.x.
65. **Rietschel ET, Kirikae T, Schade FU, Mamat U, Schmidt G, Loppnow H, Ulmer AJ, Zahringer U, Seydel U, Di Padova F, et al.** 1994. Bacterial endotoxin: molecular relationships of structure to activity and function. FASEB J. **8:**217–225.
66. **Usacheva MN, Teichert MC, Sievert CE, Biel MA.** 2006. Effect of Ca+ on the photobactericidal efficacy of methylene blue and toluidine blue against gram-negative bacteria and the dye affinity for lipopolysaccharides. Lasers Surg. Med. **38:**946–954. http://dx.doi.org/10.1002/lsm.20400.
67. **Park JH, Ahn MY, Kim YC, Kim SA, Moon YH, Ahn SG, Yoon JH.** 2012. In vitro and in vivo antimicrobial effect of photodynamic therapy using a highly pure chlorin e6 against Staphylococcus aureus Xen29. Biol. Pharm. Bull. **35:**509–514. http://dx.doi.org/10.1248/bpb.35.509.
68. **Moon YH, Kwon SM, Kim HJ, Jung KY, Park JH, Kim SA, Kim YC, Ahn SG, Yoon JH.** 2009. Efficient preparation of highly pure chlorin e6 and its photodynamic anti-cancer activity in a rat tumor model. Oncol. Rep. **22:**1085–1091. http://dx.doi.org/10.3892/or_00000540.
69. **Cunderlikova B, Gangeskar L, Moan J.** 1999. Acid-base properties of chlorin e6: relation to cellular uptake. J. Photochem. Photobiol. B **53:**81–90. http://dx.doi.org/10.1016/S1011-1344(99)00130-X.
70. **Isakau HA, Trukhacheva TV, Zhebentyaev AI, Petrov PT.** 2007. HPLC study of chlorin e6 and its molecular complex with polyvinylpyrrolidone. Biomed. Chromatogr. **21:**318–325. http://dx.doi.org/10.1002/bmc.762.
71. **Mojzisova H, Bonneau S, Vever-Bizet C, Brault D.** 2007. The pH-dependent distribution of the photosensitizer chlorin e6 among plasma proteins and membranes: a physico-chemical approach. Biochim. Biophys. Acta **1768:**366–374. http://dx.doi.org/10.1016/j.bbamem.2006.10.009.
72. **Horibe S, Nagai J, Yumoto R, Tawa R, Takano M.** 2011. Accumulation and photodynamic activity of chlorin e6 in cisplatin-resistant human lung cancer cells. J. Pharm. Sci. **100:**3010–3017. http://dx.doi.org/10.1002/jps.22501.

73. **Efremenko AV, Ignatova AA, Grin MA, Sivaev IB, Mironov AF, Bregadze VI, Feofanov AV.** 2014. Chlorin e6 fused with a cobalt-bis (dicarbollide) nanoparticle provides efficient boron delivery and photoinduced cytotoxicity in cancer cells. Photochem. Photobiol. Sci. **13:**92–102. http://dx.doi.org/10.1039/c3pp50226k.
74. **Welin J, Wilkins JC, Beighton D, Svensater G.** 2004. Protein expression by Streptococcus mutans during initial stage of biofilm formation. Appl. Environ. Microbiol. **70:**3736–3741. http://dx.doi.org/10.1128/AEM.70.6.3736-3741.2004.
75. **Kramer-Marek G, Serpa C, Szurko A, Widel M, Sochanik A, Snietura M, Kus P, Nunes RM, Arnaut LG, Ratuszna A.** 2006. Spectroscopic properties and photodynamic effects of new lipophilic porphyrin derivatives: efficacy, localisation and cell death pathways. J. Photochem. Photobiol. B **84:**1–14. http://dx.doi.org/10.1016/j.jphotobiol.2005.12.011.